

ChemComm

Accepted Manuscript



This is an *Accepted Manuscript*, which has been through the Royal Society of Chemistry peer review process and has been accepted for publication.

Accepted Manuscripts are published online shortly after acceptance, before technical editing, formatting and proof reading. Using this free service, authors can make their results available to the community, in citable form, before we publish the edited article. We will replace this *Accepted Manuscript* with the edited and formatted *Advance Article* as soon as it is available.

You can find more information about *Accepted Manuscripts* in the [Information for Authors](#).

Please note that technical editing may introduce minor changes to the text and/or graphics, which may alter content. The journal's standard [Terms & Conditions](#) and the [Ethical guidelines](#) still apply. In no event shall the Royal Society of Chemistry be held responsible for any errors or omissions in this *Accepted Manuscript* or any consequences arising from the use of any information it contains.



Journal Name

ARTICLE

Received

00th January 20xx,

Space Science Applications for Conducting Polymer Particles: Synthetic Mimics for Cosmic Dust and Micrometeorites

Lee A. Fielding,^{a,5} Jon K. Hillier,^b Mark J. Burchell^{b,*} and Steven P. Armes^{a,*}

Accepted 00th January 20xx

DOI: 10.1039/x0xx00000x

www.rsc.org/

Over the last decade or so, a range of polypyrrole-based particles have been designed and evaluated for space science applications. This electrically conductive polymer enables such particles to efficiently acquire surface charge, which in turn allows their acceleration up to the hypervelocity regime ($> 1 \text{ km s}^{-1}$) using a Van de Graaff accelerator. Either organic latex (e.g. polystyrene or poly(methyl methacrylate)) or various inorganic materials (such as silica, olivine or pyrrhotite) can be coated with polypyrrole; these core-shell particles are useful mimics for understanding the hypervelocity impact ionisation behaviour of micro-meteorites (a.k.a. cosmic dust). Impacts on metal targets at relatively low hypervelocities ($< 10 \text{ km s}^{-1}$) generate ionic plasma composed mainly of *molecular* fragments, whereas higher hypervelocities ($> 10 \text{ km s}^{-1}$) generate predominately *atomic* species, since many more chemical bonds are cleaved if the particles impinge with higher kinetic energy. Such fundamental studies are relevant to the calibration of the cosmic dust analyser (CDA) onboard the *Cassini* spacecraft, which was designed to determine the chemical composition of Saturn's dust rings. Inspired by volcanism observed for one of the Jupiter's moons (Io), polypyrrole-coated sulfur-rich latexes have also been designed to help space scientists understand ionisation spectra originating from sulfur-rich dust particles. Finally, relatively large ($20 \mu\text{m}$ diameter) polypyrrole-coated polystyrene latexes have proven to be useful for understanding the extent of thermal ablation of organic projectiles when fired at ultralow density aerogel targets at up to 6.1 km s^{-1} using a Light Gas Gun. In this case, the sacrificial polypyrrole overlayer simply provides a convenient spectroscopic signature (rather than a conductive overlayer), and the scientific findings have important implications for the detection of organic dust grains during the *Stardust* space mission.

Background: Organic Conducting Polymers

Most conventional polymers are electrical insulators and many applications make use of such properties (e.g. plastic coatings for cables and wires, printed circuit boards, etc). Although the subject of various isolated research papers stretching back over a hundred years or more,¹⁻⁵ organic conducting polymers were only recognised as a distinct class of materials since the Nobel Prize-winning discovery of highly conducting polyacetylene in 1977.⁶ Over the last twenty years or so, conducting polymers have become essential components in organic solar cells, polymer-based light emitting diodes and polymer lasers.⁷⁻⁹ The essential pre-requisites for an electrically conductive polymer are an extensively conjugated backbone and mobile charge carriers (i.e. holes or electrons). Prototype conducting polymers such as polyacetylene suffer

from significant chemical degradation: the highly conjugated backbone is readily attacked by aerial oxygen and/or water, leading to rapid conductivity decay over time scales of hours to days.¹⁰ In contrast, polyheterocycles such as polypyrrole (PPy) or poly(3,4-ethylenedioxy-thiophene) (PEDOT) exhibit much better long-term conductivity stability than polyacetylene, whereas polymeric quaternary ammonium salts such as polyaniline (PANi) are completely air-stable over time scales of years.¹¹⁻¹³

In this review article, our focus is on PPy, PANi and PEDOT (see chemical structures in Figure 1), with particular emphasis being placed on the former material. The chemical synthesis of each of these polymers involves oxidation polymerisation, typically in aqueous acidic solution.¹⁴⁻¹⁶ In the absence of a suitable stabiliser, the conducting polymer is obtained as an insoluble bulk powder of very limited processability.[‡]

The polypyrrole chains are both lightly cross-linked and highly conjugated. The latter properly gives rise to the intensely black colouration of this material and the delocalised positive charge along its backbone (there is typically one 'hole' per 3 to 4 polymerised pyrrole rings) leads to solid-state electrical conductivities of approximately $1\text{-}10 \text{ S cm}^{-1}$, as judged by four-point probe measurements conducted on pressed pellets at room temperature. This places polypyrrole within the metallic regime ($> 1 \text{ S cm}^{-1}$); its conductivity is comparable to a high-

^a Department of Chemistry, University of Sheffield, Brook Hill, Sheffield, South Yorkshire, S3 7HF, UK.

^b Department of Space Science, School of Physical Sciences, Ingram Building, University of Kent, Canterbury, Kent, CT2 7NH, UK.

⁵ Present address: School of Materials, University of Manchester, Oxford Road, Manchester, M13 9PL, UK.

* Authors to whom correspondence should be addressed (polymer chemistry queries to s.p.arnes@sheffield.ac.uk; space science queries to m.j.burchell@kent.ac.uk).

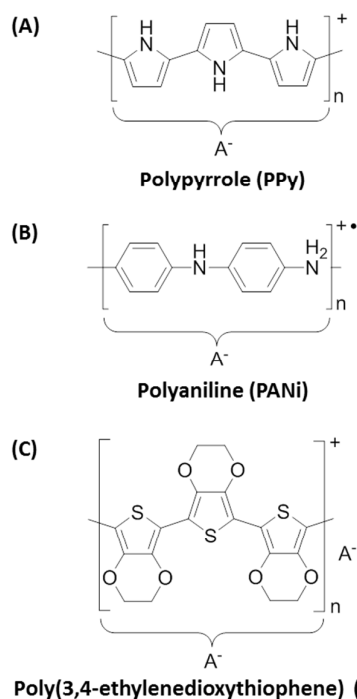


Figure 1. Chemical structures of doped forms of (A) PPy, (B) PANi and (C) PEDOT.

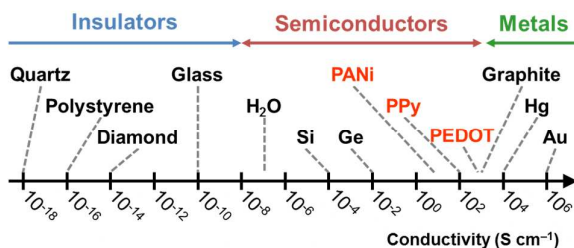


Figure 2. Conductivity chart (log scaled) showing approximate conductivities of doped forms of PANi, PPy, PEDOT and a selection of metals, semiconductors and insulators.

quality carbon black, but significantly lower than conventional metals such as copper or silver (see Figure 2). The two main reasons for choosing polypyrrole as a projectile material (rather than, say, carbon black or metals) are: (i) its convenient synthesis in the form of colloidal particles of tuneable size; (ii) the ease of coating various colloidal substrates (latexes, inorganic oxides, mineral grains etc.) with a contiguous polypyrrole overlayer from aqueous solution at room temperature. Generally, FeCl_3 is preferred for the polymerisation of pyrrole.¹⁴ This oxidant gives a product with a relatively high conductivity and its rate of polymerisation is slow enough to be compatible with a wide range of colloidal formulations. In contrast, $(\text{NH}_4)_2\text{S}_2\text{O}_8$ is a much stronger oxidant that can often introduce carbonyl defects into the polymer backbone, as confirmed by FT-IR spectroscopy studies.^{17, 18} Such over-oxidation leads to lower conductivities by up to an order of magnitude. Moreover, the kinetics of polymerisation of pyrrole is much faster when using $(\text{NH}_4)_2\text{S}_2\text{O}_8$ with polymerisations often being complete within a few

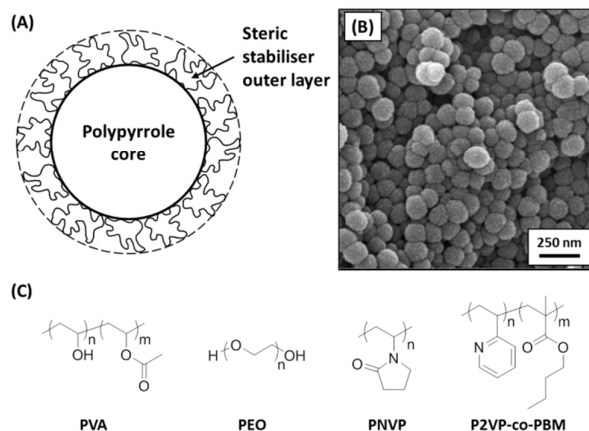


Figure 3. (A) Schematic cartoon of sterically-stabilised PPy particles, (B) TEM image of PNVP-PPy particles prepared using ammonium persulfate, (C) chemical structure of PVA, PNVP, PEO and P2VP-co-PBM steric stabilisers.

minutes at room temperature (rather than typically 12–24 h for FeCl_3 -mediated polymerisations).^{19, 20} This is simply too fast for some colloidal formulations, resulting in partial or complete precipitation of the PPy particles. Nevertheless, $(\text{NH}_4)_2\text{S}_2\text{O}_8$ can still be a *preferred* oxidant in some cases. For example, when coating certain delicate substrates that are known to be susceptible to over-oxidation, it may be preferable to use $(\text{NH}_4)_2\text{S}_2\text{O}_8$ in order to minimise the contact time of the substrate with the acidic oxidising solution (see later). In such cases, excess pyrrole monomer can be employed to ensure that all of the oxidant is consumed and the oxidant can be added last to the reaction mixture so as to minimise any oxidative surface degradation of the mineral grains.

Over the last decade or so, we have examined four classes of conducting polymer-based particles as putative mimics for understanding the behaviour of various types of micro-meteorites (a.k.a. ‘cosmic dust’) in space science experiments. Here the relatively high electrical conductivity of the particles is critical because it allows efficient accumulation of surface charge. This in turn enables the particles to be accelerated up to very high velocities (see later), which correspond to those attained by micro-meteorites within our Solar System. This provides space scientists with the opportunity to conduct fundamental laboratory-based experiments on model dust particles with relatively narrow size distributions under carefully controlled conditions at velocities similar to those encountered in space. The synthetic routes utilised to produce each class of conducting polymer particles are discussed in turn below.

Sterically-Stabilised Polypyrrole Latexes

If the polymerisation of pyrrole is conducted in the presence of a suitable water-soluble polymer, colloidal polypyrrole particles can be produced by a process known as aqueous dispersion polymerisation. Initially, the monomer, oxidant and polymeric stabiliser are soluble in the aqueous phase. As the conducting polymer is formed, the polymeric stabiliser adsorbs

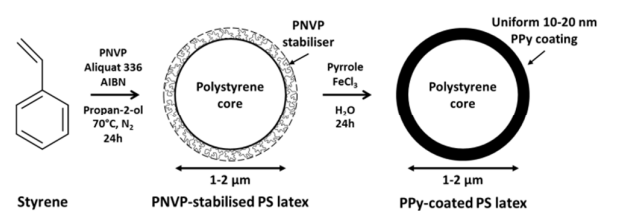


Figure 4. Schematic representation of the synthesis of PNVP-stabilised PS latex via alcoholic dispersion polymerisation, followed by PPy deposition onto the latex surface.

onto the microscopic precipitating nuclei, preventing their further aggregation by a mechanism known as steric stabilisation. The result is an aqueous dispersion of sterically-stabilised polypyrrole latexes (see Figure 3). Typically, the polymeric stabiliser is merely physically adsorbed onto the surface of the polypyrrole particles via either hydrogen bonding²¹ or electrostatics,²² although chemically-grafted stabilisers have also been developed,^{23, 24} this latter approach has not yet been utilised for space science applications. The biocompatible nature of polypyrrole, coupled with its intense intrinsic pigmentation and strong absorption of near-IR radiation, has led to various biomedical applications being explored for such polypyrrole-based nanoparticles.²⁵⁻³²

One of the most convenient, albeit empirical, methods for adjusting the mean particle size of sterically-stabilised polypyrrole latexes is simply to vary the nature of the steric stabiliser.³³ Thus using poly(vinyl alcohol) typically affords polypyrrole latexes of approximately 100 nm diameter, whereas a poly(2-vinylpyridine)-based stabiliser yields particles with a mean diameter of around 200 nm and utilising a high molecular weight poly(ethylene oxide) produces 300 nm particles. In each case relatively narrow particle size distributions are typically obtained, as judged by charge-velocity analysis studies.³³

The stabiliser content of such polypyrrole latexes typically depends on both the latex diameter and the stabiliser type. Smaller, higher surface area latexes tend to contain more stabiliser, but stabiliser contents are rarely above 10 % by mass. Thus the majority of the latex (> 90 %) comprises the electrically conductive polypyrrole cores. XPS studies suggest that the stabiliser overlayer becomes rather patchy on drying these latex particles.²² Thus the underlying polypyrrole cores are exposed, which allows sufficient charge to be accumulated to enable efficient electrostatic acceleration using a Van de Graaf instrument (see later).³⁴

Polypyrrole-Coated Latexes

Although the mean diameter of sterically-stabilised polypyrrole latexes can be readily varied, it is not possible to prepare micrometer-sized particles by this route. Instead, near-monodisperse, micrometer-sized sterically-stabilised polystyrene latexes can be prepared by non-aqueous dispersion polymerisation,³⁵ followed by the controlled deposition of an ultrathin polypyrrole overlayer onto these particles from aqueous solution³⁶⁻³⁹ (see Figure 4). It is

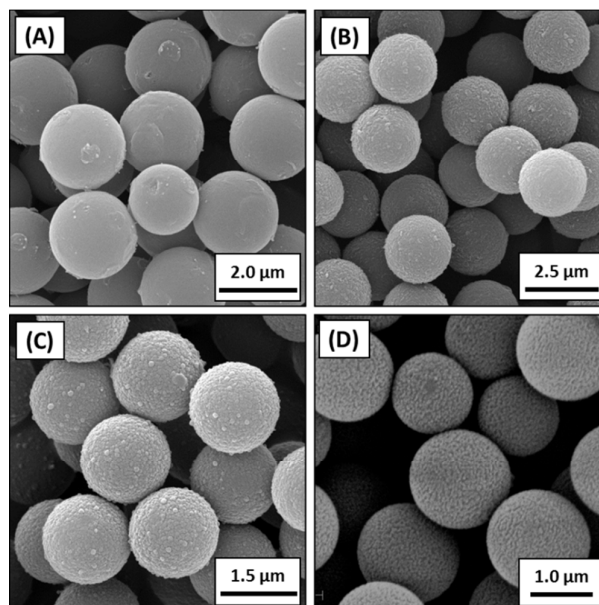


Figure 5. SEM images of (a) pristine 2.1 µm PNVP-stabilised PS latex (b) 2.3 µm PS latex coated with 10.6 wt. % PEDOT (c) 1.8 µm PS latex coated with 12.7 wt. % PPy (d) 1.6 µm PS latex coated with 9.5 wt. % PANI.

important to determine the specific surface area of the original polystyrene latex by an appropriate technique such as BET surface area analysis.³⁸ From the latex mass utilised, the total latex surface area can be readily calculated for a given formulation. Thus, given the densities of the latex (ρ_{latex}) and the conducting polymer (ρ_{PPy}), the latex mass (M_{latex}) and the mean latex radius (R_{latex}), this information enables the approximate polypyrrole mass loading (M_{PPy}) required to produce a particular polypyrrole overlayer thickness (x) to be determined using equation 1.³⁸

$$x = R_{latex} \left[\left(\frac{M_{PPy} \rho_{latex}}{M_{latex} \rho_{PPy}} + 1 \right)^{1/3} - 1 \right] \quad (1)$$

In practice, this approach is limited to overlayer thicknesses of around 1-30 nm. If much thicker overlayers are targeted, the conducting polymer coating becomes rather inhomogeneous and the deposition process is much less well controlled, with some macroscopic precipitation of the conducting polymer usually observed. However, optimised protocols invariably lead to well-defined 'core-shell' particles with electrically insulating cores and electrically conductive shells, with typical polypyrrole loadings of 1-10 % by mass depending on the mean latex diameter and the desired shell thickness. This robust protocol was subsequently extended to include somewhat larger polystyrene latex particles of 20 µm.⁴⁰ Scanning electron microscopy studies indicate that the polypyrrole overlayer is relatively smooth and uniform (see Figure 5c). Solvent extraction experiments confirm that the overlayer is both robust and contiguous, since a 'goldfish bowl' morphology is observed for the insoluble polypyrrole residues

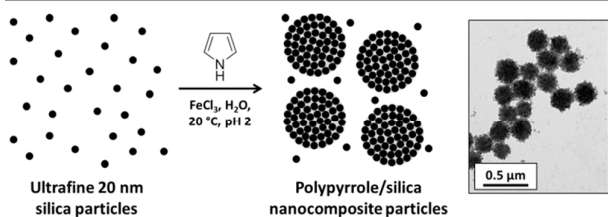


Figure 6. Schematic representation of the synthesis of polypyrrole/silica nanocomposite particles by oxidative polymerisation of pyrrole in the presence of an aqueous silica sol. A representative TEM image of polypyrrole/silica nanocomposite particles is shown on the right.

after all the underlying polystyrene latex has been removed. This protocol can also be used to coat submicrometer-sized latex particles.^{41, 42} The same approach also works reasonably well for the deposition of PANi and PEDOT, but in these cases the deposited conducting polymer overlayer tends to be somewhat less uniform⁴³⁻⁴⁵ (see Figure 5b and 5d). Use of less hydrophobic latexes such as poly(methyl methacrylate) particles also tends to produce relatively inhomogeneous conducting polymer coatings⁴⁶ (see Figure 13a).

Polypyrrole/Silica Nanocomposite Particles

If pyrrole is polymerised in the presence of an ultrafine 20 nm silica sol in aqueous solution under appropriate conditions, then polypyrrole/silica nanocomposite particles are formed with little or no macroscopic precipitation^{17, 47-49} (see Figure 6). The conducting polymer chains adsorb onto the silica nanoparticles and bind them together to form colloiddally stable aggregates. Excess silica sol is readily removed by repeated centrifugation-redispersion cycles and the purified polypyrrole/silica nanocomposite particles can then be characterised by various techniques. Their surface compositions are invariably silica-rich as judged by X-ray photoelectron spectroscopy⁵⁰ and aqueous electrophoresis⁵¹, which no doubt accounts for their excellent long-term colloid stability. Thermogravimetric analysis readily provides the mean silica contents of such nanocomposite particles. Alternatively, elemental microanalyses can be used to calculate the organic content of the nanocomposite particles (using polypyrrole bulk powder as a reference material), with the silica content then being obtained by subtraction. It is possible to vary the mean nanocomposite diameter and also the mean silica content, but these two synthesis parameters appear to be inter-dependent.^{17, 47} Thus using the FeCl_3 oxidant typically produces larger polypyrrole/silica nanocomposite particles of 250-300 nm diameter and relatively low silica contents (30-40 % by mass) whereas using $(\text{NH}_4)_2\text{S}_2\text{O}_8$ oxidant invariably leads to smaller nanocomposite particles of 110-180 nm comprising 50-60 % silica. Both electron microscopy and disc centrifuge photosedimentometry indicate that relatively narrow size distributions are obtained in each case. Given the electrically insulating nature of the silica component, solid-state conductivities for these nanocomposite particles are generally somewhat lower than

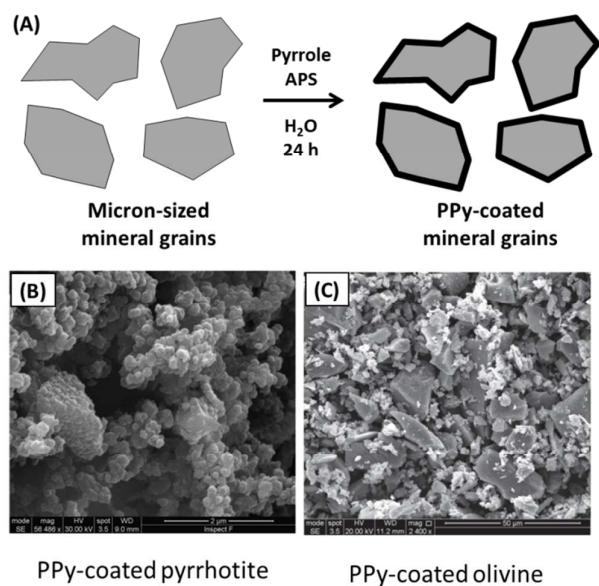


Figure 7. (A) Schematic representation for the coating mineral grains with PPy. SEM images of (B) PPy-coated pyrrhotite grains and (C) PPy-coated olivine grains. Image B was adapted from Hillier et al.,⁵² Figure 3 and image C was adapted from Postberg et al.,⁵³ Figure 3b.

for the other colloidal forms of polypyrrole, ranging from 10^{-3} to 10^0 S cm^{-1} . Nevertheless, this is sufficient to allow the accumulation of sufficient surface charge to enable acceleration up to hypervelocities (see later). This general approach has also been extended to include ultrafine tin(IV) oxide nanoparticles instead of silica sols.⁵⁴ In this case, somewhat higher electrical conductivities can be achieved, particularly if the tin(IV) oxide component is doped with antimony in order to render it semi-conductive.⁵⁵

Polypyrrole-Coated Mineral Grains

Various mineral grains (e.g. olivine, pyroxene, pyrrhotite, aluminosilicates etc.) can be conveniently coated with an ultrathin overlayer of polypyrrole by simply using the same formulation developed to coat latex particles (see above) and substituting the mineral grains for the latex particles (see Figure 7A). Again, knowledge of the 'sphere-equivalent' specific surface area and density of the mineral grains of interest is essential for calculating the mean polypyrrole overlayer thickness via Equation 1. Generally, the polypyrrole overlayer is not quite as uniform as that achieved for the latex particles, but it is usually sufficient for acceleration up to hypervelocities. The mineral grains are usually obtained by grinding up the corresponding macroscopic material, so they often have rather polydisperse and ill-defined particle morphologies (see Figures 7b and 7c). Nevertheless, such projectiles are of considerable interest to space scientists, since their chemical compositions often closely match those of known micro-meteorites and cosmic dust.^{52, 56} In the case of certain minerals such as pyrrhotite,⁵² the oxidising conditions used for polypyrrole deposition may be detrimental to their

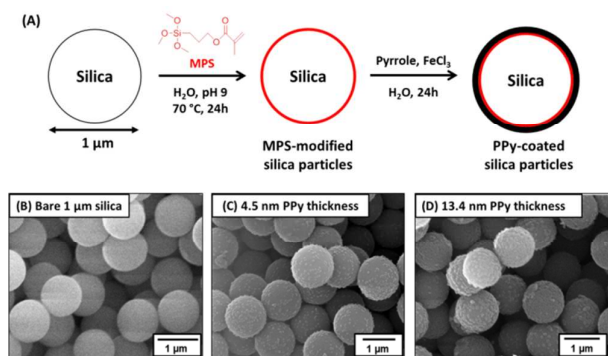


Figure 8. (A) PPy deposition onto 1 μm silica particles, SEM images of (B) bare silica, (C+D) silica with increasing PPy thickness. Schematic and images adapted from Lovett *et al.*⁵⁷

chemical stability. In this case, it is preferable to use $(\text{NH}_4)_2\text{S}_2\text{O}_8$ as the oxidant rather than FeCl_3 since this ensures much shorter reaction times (just a few minutes, rather than many hours). In addition, the oxidant is added last to the reaction mixture in order to minimise chemical degradation of the mineral grains. Selected electron micrographs for various polypyrrole-coated mineral grains are shown in Figure 7B and 7C.

Notwithstanding the synthesis of polypyrrole/silica nanocomposite particles described above, it is relatively difficult to coat large silica particles with an ultrathin contiguous overlayer of polypyrrole.⁵⁸ This is because the highly anionic silica surface is relatively hydrophilic, and polypyrrole does not readily 'wet' such substrates, leading to an inhomogeneous, non-uniform coating.⁵⁹ This problem has been recently addressed by surface modification of near-monodisperse silica particles of approximately 1 μm diameter using a commercial organosilane reagent, 3-(methacryloyl)propyl triethoxysilane.⁵⁷ This increases the surface wettability of the silica particles and hence enables much more uniform deposition of the polypyrrole overlayer, as judged by scanning electron microscopy (see Figure 8). The resulting polypyrrole-coated silica particles can be accelerated up to 7-9 km s^{-1} using a Van de Graaff instrument³⁴ (see later) and have been used as model projectiles to generate crater impacts in aluminium foils at various angles of incidence.^{56, 60}

Other Conducting Polymer Colloids

Although the vast majority of our studies have been conducted using polypyrrole-based projectiles, there are at least two viable alternatives to this conducting polymer. Both polyaniline (PANI) and poly(3,4-ethylenedioxythiophene) (PEDOT) have been prepared in the form of sterically-stabilised latexes^{61, 62} as ultrathin coatings on latex particles⁴³⁻⁴⁵ or as colloidal nanocomposite particles using an ultrafine silica sol.^{63, 64} However, such syntheses are generally more demanding than the analogous colloidal polypyrrole systems. For example, the preparation of sterically-stabilised PANi particles is best conducted using a tailor-made reactive polymeric stabiliser, while PEDOT syntheses work best (but are still relatively

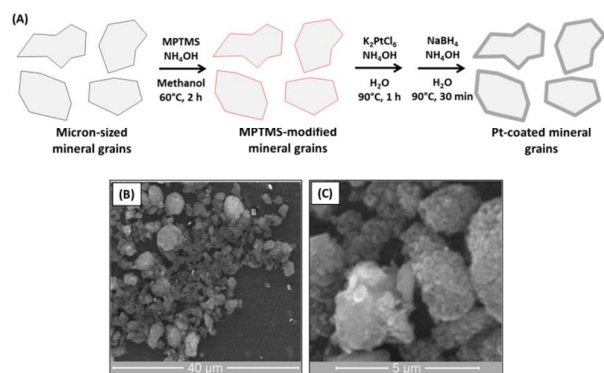


Figure 9. (A) Schematic showing the electroless deposition of metals (Pt) onto mineral grains. (B and C) SEM images of Pt-coated silica particles. Images B and C are adapted from Hillier *et al.*,⁶⁵ Figures 1 and 2.

inefficient) when conducted at elevated temperatures using a ferric 4-toluenesulfonate oxidant, which is not commercially available. At first sight, this appears to be unfortunate, since both PANi and PEDOT offer superior long-term conductivity stability compared to polypyrrole. However, PVA-stabilised polypyrrole particles stored under ambient conditions for more than ten years can still acquire sufficient surface charge to enable their acceleration up to the hypervelocity regime.⁶⁶ Thus any additional chemical stability that may be conferred by either PANi or PEDOT does not appear to offer a decisive advantage.⁵

An Alternative Approach to Conducting Polymer Deposition: Surface Metallisation

Recently, surface metallisation of electrically insulating projectiles using colloidal precious metal seeds has been reported.⁶⁵ It has enabled silica nanoparticle agglomerate dust particles of 0.1-1.0 μm diameter to be coated with platinum, which is sufficient to enable the projectiles to be accelerated to hypervelocities ranging from 4 to 30 km s^{-1} in Van de Graaff experiments. More recently, the same approach has been utilised to coat anorthite, mixed-silicate (predominantly orthopyroxene) particles as well as olivine particles (Figure 9).^{53, 67, 68} In principle, much more cost-effective metals such as Sn or Ag should enable deposition of low-density metallic overlayers and such approaches are actively being developed. One important advantage of the metallisation approach is that such coatings produce ionic plasmas that contain simple metal cations which can be readily identified by mass spectroscopy. In contrast, the conducting polymer coatings can fragment to form a range of molecular and/or atomic ions, depending on the impact velocity.⁵² As discussed above, studies of such ionic plasmas from organic particles usually indicate that their mass spectra are typically dominated by e.g. the latex core, rather than the coating material. However, more recent experiments^{52, 69} have shown that, at least in the case of impact velocities below approximately 30 km s^{-1} , molecular fragments originating from the polypyrrole coating can contribute to the plasma mass spectra, which depending on

the resolution of the mass spectrometer used, complicates their interpretation. In this context surface metallisation appears to offer a useful alternative approach to deposition of an organic conducting polymer. However, the relatively high density of platinum ($\sim 22 \text{ g cm}^{-3}$) means that the density of the coated particles will be significantly higher than the precursor particles, even when targeting metallic overlayers of just 5–20 nm. In contrast, the relatively low densities of conducting polymers ($\sim 1.50 \text{ g cm}^{-3}$) actually results in a slight *reduction* in particle density for most mineral grains, as well as a far smaller increase in mass. Conducting polymer-coated projectiles are therefore best suited to hypervelocity experiments which are highly sensitive to particle mass and/or density, such as those investigating impact charge, crater or aerogel track morphology.

Hypervelocity Experiments

Most of the cosmic dust particles commonly found in our Solar System fall into one of the following four categories: metallic, silicate-rich, carbonaceous or icy. The former class can be readily mimicked using finely divided metal powders or metal sols. For example, experimental studies often focus on iron particles,^{34, 70, 71} since their high intrinsic conductivity enables efficient charging and acceleration up to hypervelocities. However, the other three classes of cosmic dust are primarily electrical insulators and for many years none of these materials were suitable for laboratory-based electrostatic acceleration hypervelocity experiments.⁵⁵ The use of electrostatic acceleration is necessary when velocities higher than approximately 7 km s^{-1} or precise control of the particle flux or mass are required. For lower velocities, or the acceleration of multiple grains simultaneously, a light gas gun may be used,³⁴ which does not require charge-carrying cosmic dust analogues. Advances in the field of conducting polymers have allowed a range of synthetic carbonaceous projectiles to be developed, while conducting polymer coatings have enabled various other mineral grains to be accelerated up to hypervelocities⁵³ in electrostatic Van de Graaff accelerators. The first report of the acceleration of conducting polymer-based particles up to the hypervelocity regime ($> 1 \text{ km s}^{-1}$) was by Armes et al.³³ A series of sterically-stabilised polypyrrole particles were evaluated in turn and charge-velocity analysis used to determine their particle size distributions using a small scale 20 kV 'test bench' accelerator that allowed velocities of up to 5 km s^{-1} to be achieved. This approach enables particles to be accelerated into the hypervelocity regime using the well-established principle of electrostatic acceleration, confirming the suitability of the particles and their coating for use in the larger accelerators, to which access may be limited for purely testing and characterisation purposes. The relation, $qV = \frac{1}{2}mv^2$, where q is the particle charge, V is the applied voltage, m is the particle mass and v its velocity, governs the mass-velocity space in which cosmic dust analogues may be electrostatically accelerated. According to this equation, increasing the applied electric field leads to a corresponding increase in the maximum velocity that can be

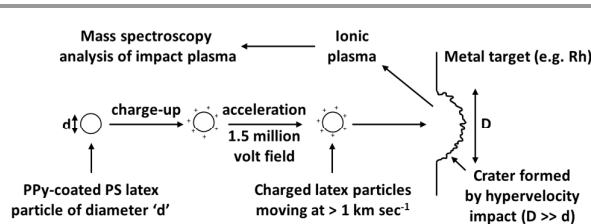


Figure 10. Schematic representation showing the main events during a typical hypervelocity impact experiment. Adapted from Khan et al.,⁷² Figure 3.

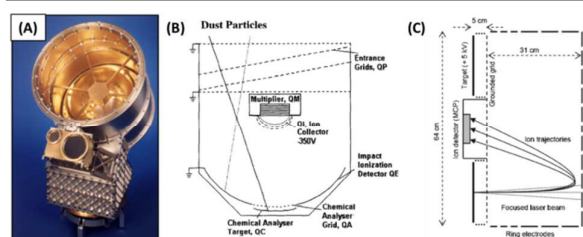


Figure 11. (A) Digital image and (B) schematic of the cosmic dust analyser on board Cassini and (C) schematic of the LAMA spectrometer. Image A adapted from Srama et al.,⁷³ Figure 1, schematic B adapted from Goldsworthy et al.,⁷⁰ Figure 2 and schematic C adapted from Sternovsky et al.,⁷⁴ Figure 1.

achieved for a given projectile. In practice a high field strength Van de Graaff accelerator is required to obtain hypervelocities, with accelerators currently in use utilising potential differences of between 2.0 MV⁷⁵ and 3.0 MV.⁷⁶ Accurate measurement of the charge carried by individual grains (via induction and charge amplification) and the velocities of the grains (via induction detectors separated by an accurately known distance^{34, 77, 78}), combined with the known acceleration voltage allows the particle mass to be determined. If the grain density is also known then its equivalent spherical radius may be estimated.

For example, a 130 nm diameter polypyrrole particle (whose mass is approximately $1.68 \times 10^{-18} \text{ kg}$) with a charge of $6.49 \times 10^{-16} \text{ C}$, accelerated through a 2.0 MV applied field can attain a hypervelocity of up to 39.3 km s^{-1} (approximately 88000 mph).⁷⁰ As far as we are aware, this is the highest velocity ever reported for a synthetic organic projectile.

Impact Ionisation Experiments

The enormous energy density of a conducting polymer-based projectile impinging on a metal target at more than a few km s^{-1} is sufficient to cause extensive bond scission, as well as ionisation (Figure 10).⁷² This leads to the formation of ionic plasma that can be interrogated by time-of-flight mass spectroscopy or charge integrators. The instruments used for mass spectroscopy are typically duplicates of mass spectrometers on-board various spacecraft. As such, their mass resolution is much lower than state-of-the-art analytical mass spectrometers, due to the highly restrictive limitations of size, weight and energy consumption that are necessarily placed on space instrumentation. Nevertheless, space instruments such as the Cosmic Dust Analyser [CDA]⁷³ on-board the *Cassini* spacecraft are capable of discriminating

between ions with a mass-dependent mass resolution ($m/\Delta m$) of approximately 50.

Typically, the impact plasma is separated using an applied electric field (e.g. 330 kV m^{-1} in CDA), with either the cation or anion component accelerated towards an ion detector, through a low-field, or field-free region. In recent years, higher resolution mass spectrometers, designed for space-based operation and capable of detecting both positively and negatively charge plasma components, have been developed [e.g. the Large Area Mass Analyser, LAMA]^{74, 79} (Figure 11). These spectrometers use a more complicated field geometry (reflectron⁸⁰) within the instrument to remove the effects of the ions' initial energies within the impact plasma, as well as provide a longer ion trajectory, and thus increase the mass resolution of the instrument ($m/\Delta m \approx 200$).⁷⁴ In both the drift and reflectron cases, the ions' detection times (t_i) are related to their masses (m_i) and charges (q_i) by $t_i = a(m_i/q_i)^{0.5} + b$, where 'a' is known as the stretch parameter, related to the electric field geometry and strength within the instrument and 'b' is known as the shift parameter, related to the instrument recording trigger time. In the case of unknown a and b , spectra can be calibrated using two peaks of known masses (and assumed to be due to ions of the same energy) and arrival times to solve for a and b .

Both the simpler, CDA-type mass spectrometers and the more complex LAMA-type utilise the plasma generated^{81, 82} during the rapid deceleration of particles travelling at hypervelocities (defined in this case as a velocity higher than the speed of sound in both target and projectile). The energies involved produce an impact cloud, typically composed of macroscopic ejecta, neutral and charged molecules and atoms as well as electrons. The plasma generated during a hypervelocity impact has components due to both the impinging projectile and the target that is struck. It is important to test this impact ionisation phenomenon experimentally as there is a limited understanding of how it works as a function of impact speed and associated shock pressures. The behaviour of most materials, e.g. to what degree they ionise, in what form they will show up in mass spectra etc., thus has to be determined experimentally.

At low ($< 5 \text{ km s}^{-1}$) velocities, the charged particles produced are typically due to easily ionised species, such as alkali metals (e.g. Na, K) or species with a high electron affinity (e.g. CN in the case of organics) (Figure 12A). Increasing the impact velocity to between 5 km s^{-1} and approximately 15 km s^{-1} results in the production of additional species, both atomic (e.g. C, O, Si, S) and molecular (e.g. C_2H_3 , C_2H_5), with decreasing molecular weights at higher velocities. Between $20\text{--}30 \text{ km s}^{-1}$ molecular organic cations become far less frequent, although molecular organic anions are still present. Above approximately 30 km s^{-1} the impact cloud is dominated by atomic ions. Examples of mass spectra showing the progression from molecular to atomic species in the plasma can be seen for metal-coated particles⁶⁷ and organic-rich, polymer-coated particles.^{52, 70, 83, 84}

Impact ionisation mass spectrometry using purely organic particles is designed to investigate and simulate mass spectra

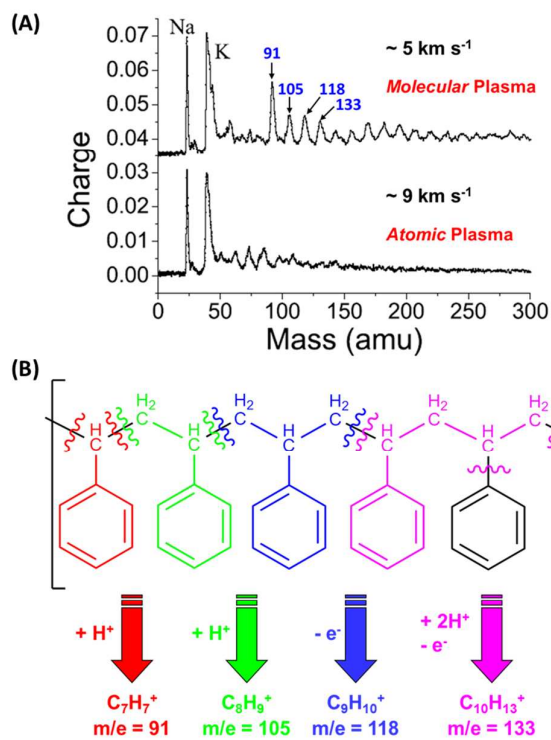


Figure 12. (A) Impact ionisation spectra of PPy-coated PS microparticles onto rhodium at 5 and 9 km s^{-1} (B) Fragmentation scheme for the typical cation fragments observed, resulting from cleavage of aromatic rings from polystyrene. Graph A adapted from Goldsworthy et al.,⁷⁰ Figure 10.

which would be generated by organic-rich particles. These particles may come from various sources^{85, 86}, including carbonaceous chondrites (i.e. from asteroids⁸⁷ within the solar system), organic dusts from cometary sources,^{87, 88} or the tholin-rich⁸⁹ processed surfaces of volatile-rich bodies such as Centaurs⁹⁰ or trans-Neptunian objects⁹¹, and finally polyaromatic hydrocarbon-rich dust originating from outside the solar system.^{92, 93} As well as their compositional similarity to such organic-rich grains, the synthetic polymer particles also possess relatively low densities ($< 1500 \text{ kg m}^{-3}$). This is comparable to that of water ice or "fluffy" aggregate grains, such as those identified during the *Stardust* Interstellar Preliminary Examination.⁹⁴

Experiments performed using purely organic projectiles and a laboratory model of CDA with a Rh target,^{70, 84} prior to the arrival of *Cassini* in the Saturnian system, were designed to investigate the mass spectra of carbonaceous grains which may have been intercepted during *Cassini's* cruise phase. Polypyrrole and PEDOT-coated latexes, as well as pure polypyrrole particles, were accelerated over a range of impact velocities, with cation mass spectra recorded. These spectra show the evolution of the species produced with increasing impact velocity, as well as identifying many important charged molecular fragments, including the stable tropylium ion at a mass of 91 u (see Figure 12B).⁷⁰

Later experiments using a laboratory model of the LAMA investigated cation mass spectra of polypyrrole-coated

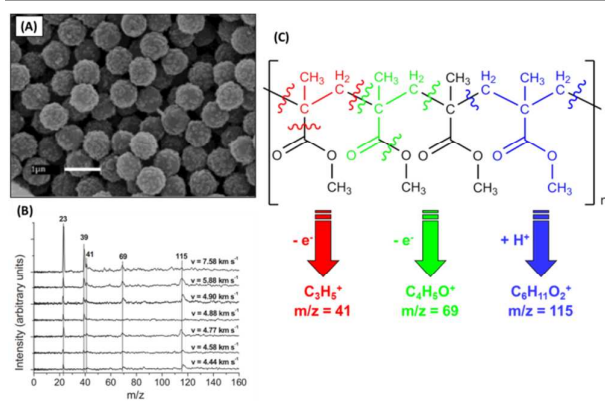


Figure 13. (A) SEM image of 740 nm PMMA latex coated with 10.5 wt. % PPy. (B) Impact ionisation mass spectra obtained for these particles impacting on a rhodium target at 4.4 – 7.6 km s⁻¹. (C) Fragmentation scheme for the typical cation fragments observed. Image A adapted from Cairns et al.,⁴⁶ Figure 2c, graph B and schematic C adapted from Burchell et al.,⁹⁵ Figures 3 and 11.

polystyrene, PANi and PMPV latexes, as well as anion mass spectra of polypyrrole-coated PMPV latex.⁶⁹ These mass spectra were produced by impacts onto an Ag target, whose large area is designed for the detection of cosmic dust in extremely low flux environments.^{74, 79} Impacts were performed over an impact velocity range of 3–35 km s⁻¹, with the large molecular fragments which survived at impact velocities below 10 km s⁻¹ found to be best suited to the identification of the parent organic species. Data collected at higher (10–35 km s⁻¹) was however also found to be useful.

The chemical structure, as well as the specific composition, of the organic material involved in an impact affects the molecular fragments produced. This effect was investigated by comparing mass spectra produced by impacts of polypyrrole-coated PMMA latex, an aliphatic compound, with those produced by impacts of polypyrrole-coated PS latex, an aromatic compound.⁹⁵ Such aliphatic compounds are good mimics of aliphatic organic species found in carbonaceous chondrites. Impacts onto a Rh target, at 4–8 km s⁻¹, of PMMA particles resulted in mass spectra exhibiting fewer large molecular species than those found in mass spectra of the PS latex particles at the same speeds. This is in agreement with predictions based upon the known thermal fragility of the PMMA compared with that of PS (Figure 13). In particular, for the aliphatic microparticles there is no distinctive signal at 91 amu, which has been previously attributed to the tropylium cation, C₇H₇⁺.^{70, 96} Instead, cationic molecular fragments are observed at 41, 65 and 115 amu, which are traceable to specific bond scissions in the chemical structure of poly(methyl methacrylate).

Although these works used solid metallic targets (albeit with some degree of organic contamination, as described in Postberg et al.⁹⁷) experiments have also been performed investigating the species produced by sulphur-rich polypyrrole-coated organic projectiles⁴¹ impacting porous metal (Ag, Au) targets at velocities of up to 30 km s⁻¹.⁸³ The targets comprised highly porous nanostructured surfaces of relatively low density (so-called ‘metal blacks’). After the high-speed impact, latex

polymer chains were chemically degraded into molecular fragments. These fragments included both carbon- and sulfur-based species, which were detected as a series of cations and anions by time-of-flight mass spectrometry. Analysis of the mass spectra confirmed that greater chemical degradation occurred at higher velocities until only atomic ions were formed. Furthermore, ‘metal black’ targets led to greater fragmentation than more compact surfaces, which could be a consequence of much smaller impact spots.⁸³ This indicates that the formation of molecular fragments occurs during expansion from the high pressure shock state.

However, purely organic particles are less likely than those which contain some mineral component. Silicates, such as olivines and orthopyroxenes form a major component of both asteroidal and cometary dust within the solar system,^{98, 99} and that found in the Interstellar Medium and dust-forming regions.^{94, 100} Early impact ionisation CDA laboratory model mass spectrometry⁷⁰ of polymer-mineral agglomerates used aluminosilicate clay nano- and microparticles, within a matrix of polypyrrole. Speeds as high as 50.7 km s⁻¹ were recorded, although the definitive identification of Al or Si in the mass spectra was complicated by the presence of organic molecular ions.

Subsequent acceleration of a simpler mineral, pyrrhotite (also coated with polypyrrole), analysed using the higher resolution LAMA instrument, showed that ionic species originating from the mineral core could be detected at velocities as low as 7 km s⁻¹.⁵² Although the suspected presence of an oxidised (and possibly hydrated) sulfate layer between the pyrrhotite and polypyrrole unexpectedly complicated the interpretation of mass spectra, organic molecular anions were detected at higher velocities than expected (>20 km s⁻¹). Several key ‘fingerprint’ molecules were identified as decomposition products of the polypyrrole backbone were also observed at masses of 66, 93 and 105 amu, which were assigned to C₄H₄N⁺, C₅H₅N₂⁺ and C₆H₅N₂⁺ cations, respectively.

Simpler instruments, such as those found on the *Ulysses*¹⁰¹ and *Galileo*¹⁰² spacecraft, measure only the amplitude and evolution of the overall charge signal produced during a hypervelocity impact. With this information, and suitable laboratory calibration, estimates of particle masses and impact velocities may be made.¹⁰³ Impacts occurring outside the Chemical Analyser Target (the Rh central target of CDA⁷³) produce very similar signals to those produced by *Galileo* and *Ulysses*, and a laboratory-based duplicate of the CDA instrument has been used for similar impact charge signal calibration.

The first impact charge signal data originating from the use of conductive polymer particles was reported by Burchell et al. in 1999.¹⁰⁴ A series of experiments with polypyrrole-, PANi- and PEDOT-coated polystyrene latexes were conducted to determine the relationship between impact velocity and the charge produced during an impact ($q = av^b$, where $b = 1.91$ – 2.02). This work was later expanded to include further polypyrrole- and PANi-coated polystyrene latexes, sterically-stabilised polypyrrole particles and also silica and tin (IV) oxide nanoparticles embedded in a polypyrrole or PANi matrix.⁶⁶

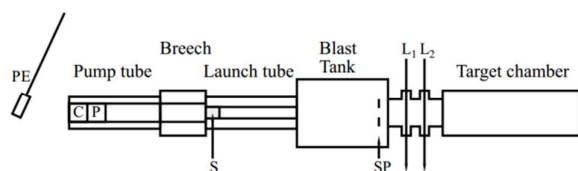


Figure 14. Schematic diagram for the light gas gun (LGG). The locations of the pendulum (PE), cartridge (C), piston (P), sabot (S), stop plate (SP) and lasers (L1 and L2) are as shown. Adapted from Burchell *et al.*,³⁴ Figure 8.

Ionisation charge yields were calculated for particles impacting Rh, Au or Cu targets, with the purely organic particles producing similar yields to those containing harder mineral grains. The majority of charge yield calibration data prior to these publications was performed using iron dust. These metallic particles produced yields similar to the lower density organic/organic-mineral grains at velocities above 10 km s^{-1} , but significantly underestimated the impact charge produced at lower velocities (by a factor of three at 5 km s^{-1} and up to a factor of ten at 1 km s^{-1}). This effect was dependent on target material, with the yield differences for Fe being smaller when using Au and Rh targets, as utilised in the space instrumentation under investigation. Ionisation charge amplitudes were again found to scale exponentially with impact velocity, with ranges of b (defined above) of 2.6 to 3.6 for speeds below 18 km s^{-1} , with one higher speed sample having $b = 6.6$, in comparison with an impact charge per unit mass scaling of $v^{3.36}$ found for iron dust.⁷⁰ Goldsworthy *et al.*⁷⁰ also presented impact charge calibration data using both polypyrrole-coated polystyrene and polypyrrole-coated aluminosilicate clay particles. The charge yield was more strongly dependent on the speed of the impinging particle than that found in the earlier work using polymer-mineral grains.

Impact Cratering and Aerogel Tracks

Impact ionisation is the only method available to study cosmic dust compositions *in situ*. Alternatively, targets passively exposed in space can be returned to Earth for study. In this case they should contain microscopic craters formed as a result of the high-speed impacts. These craters often retain residues from the impinging particles and even fine details of the crater shape (depth, diameter, etc.) can offer useful information regarding the composition, shape and structure of the impactor. Laboratory experiments to simulate such impact events typically use two-stage light gas guns (LGGs, Figure 14)^{34, 105-108} which can fire at speeds up to 8 or 9 km s^{-1} . These rely on the compression and subsequent rapid expansion of a light gas (e.g. hydrogen or helium) to propel particles up to the hypervelocity regime. In this case a conductive coating is not required for acceleration, although it may still be a useful feature (see later). Cosmic dust analogue grains are usually accelerated *en masse*, as “buckshot”, producing multiple impacts at a single speed. Although a conducting polymer overlayer is no longer essential for LGG acceleration, it has

proved useful to use the same microparticles in LGG work to understand impact cratering. This is discussed further in the following “Cometary Dust Particles” section. It is also possible to capture particles relatively intact even in impacts at a few km s^{-1} , provided that the target media has a sufficiently low density. Again, the microparticles described here have been utilised for LGG calibration experiments to better understand how capture of organic particles can alter their chemical nature.

Cassini Mission

The *Cassini* space mission to Saturn carries the Cosmic Dust Analyser discussed above and shown in Figure 11a and 11b. *Cassini* is one of NASA’s most successful multi-year missions. Launched in 1997, it swung past Jupiter in 2000 and arrived at Saturn in 2004, where it became the first spacecraft to enter orbit around Saturn. Given that the Saturnian system has a rich, complex population of dust particles, the CDA has been an essential part of the *Cassini* mission. This instrument analyses impact plasma when the dust strikes its metal Rh target at a high speed. However, it is not just sufficient to collect data, the impacts have to be correctly interpreted. This is why the microparticles described herein are so important to space science – by characterising their behaviour in laboratory experiments they have provided us with a much better understanding of the impact ionisation process. Indeed, altering the chemical compositions of these synthetic projectiles has allowed specific hypotheses to be tested regarding the likely ionisation spectra expected for various types of Saturnian dust (i.e., purely organic, mineral grains etc.).

For example, one important question for the *Cassini* mission concerned the volcanic activity of the Jovian moon Io. Io is the third largest of Jupiter’s moons and its volcanic activity has been known for more than three decades. On its journey to Saturn, *Cassini* flew past Jupiter and was thus able to investigate the dust ejected from Io. The surface colour of Io and spectroscopic analysis of its atmosphere provides strong evidence for the presence of sulfur on Io and perhaps also within its volcanic plumes. Accordingly, sulfur-containing microparticles were synthesised for hypervelocity impact experiments.^{41, 69} More specifically, dispersion polymerisation of a sulfur-rich divinyl monomer in an ethanol/water mixture, followed by coating with polypyrrole.⁴¹ Although these latexes were somewhat polydisperse in nature, they proved to be suitable mimics for sulfur-rich micro-meteorites. They could be accelerated up to $\sim 35 \text{ km s}^{-1}$ and their impact ionisation on striking a silver target led to both sulfur cations and anions being identified in the resulting ionic plasma using a LAMA detector.⁶⁹ Surprisingly, the mass spectra obtained by the CDA near Jupiter were actually dominated by NaCl, with relatively little sulfur content being detected (despite the strong evidence for sulfur on Io). Nevertheless, the observation of elemental sulfur ions in laboratory-based ionisation spectra confirms that the unexpected absence of sulfur in the spectra obtained by *Cassini* is a valid result, rather than merely an

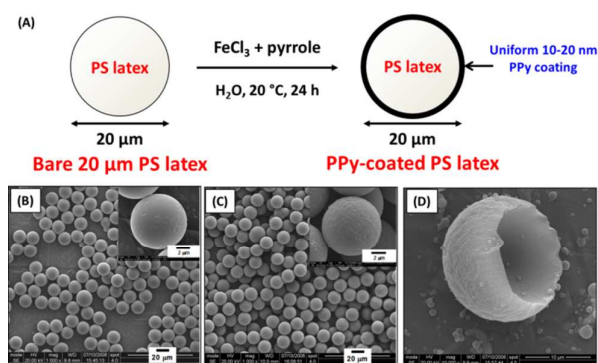


Figure 15. (A) Schematic cartoon for coating 20 µm polystyrene (PS) latex with PPy and the associated SEM images of (B) uncoated PS latex, (C) PPy-coated PS latex, (D) PPy 'goldfish bowl' after solvent extraction. Images adapted from Burchell et al.,¹⁰⁹ Figure 2.

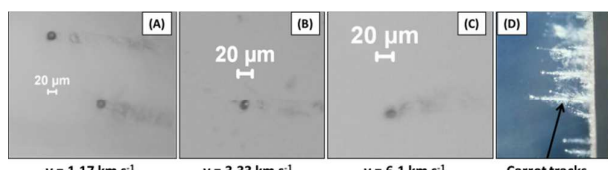


Figure 16. Digital images recorded an aerogel with captured 20 µm polystyrene microparticles coated with 20 nm polypyrrole, optical micrographs are shown for particles captured at impact speeds of (A) 1.07, (B) 3.33, and (C) 6.11 km s⁻¹. In all cases impacts were from the right, as indicated in (D). Adapted from Burchell et al.,¹⁰⁹ Figure 6.

artefact arising from a poorly understood aspect of the impact ionisation process.

Cometary Dust Particles

The *Stardust* mission was commissioned to capture dust grains emanating from comet P81/Wild-2.¹¹⁰ Launched in 1999, it flew past this comet at a relative encounter velocity of 6.1 km s⁻¹ in 2004 and returned the captured dust to Earth in 2006.¹¹¹ In addition, *Stardust* also collected potential interstellar dust grains impinging over a wide range of impact speeds.⁹⁴ As expected, a large number of dust grains were captured during the *Stardust* mission.¹¹¹ Two types of targets were used: ultralow density aerogel targets designed to provide a 'soft landing' for fast-moving grains and aluminium foils, where the impacts produced craters lined with particle residues.¹¹⁰

The use of aerogel targets to collect cosmic dust in space has been reviewed by Burchell et al.¹¹² *Stardust* utilised a transparent silica aerogel of ultralow density (ranging from 0.005 to 0.050 g cm⁻³). Particles tunnel into the aerogel during high-speed impacts and leave long, thin tracks with semi-intact dust grains located at their end. Alternatively, bulbous cavities are formed as partial break-up occurs on impact to produce many finer fragments, which line the walls of the cavity or penetrate beneath it as thin tracks. Examples of track types have been given by Hoerz et al.,¹¹³ Burchell et al.,¹¹⁴ and Trigo-Rodriguez et al.¹¹⁵ for aerogel-captured cometary dust grains. The tracks from the potential interstellar dust grains have been described by Westphal et al.¹¹⁶ Although many *inorganic*

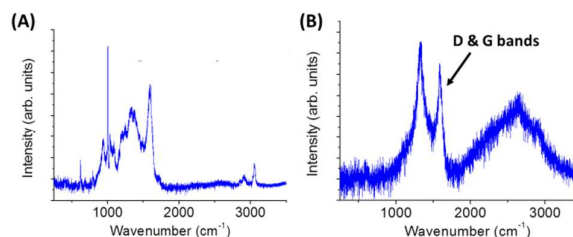


Figure 17. Raman spectra recorded *in situ* for individual PPy-coated polystyrene microparticles captured in aerogel at impact speeds of: (A) 1.07 km s⁻¹, and (B) 6.11 km s⁻¹. In (A) the spectrum resembles that of the original PPy-coated polystyrene particles. However, in (B) the distinct peaks observed in (A) have been replaced by broad bands at 1374 and 1590 cm⁻¹, which correspond to the distinctive carbon D and G bands assigned to amorphous carbon. Adapted from Burchell et al.,¹⁰⁹ Figure 9.

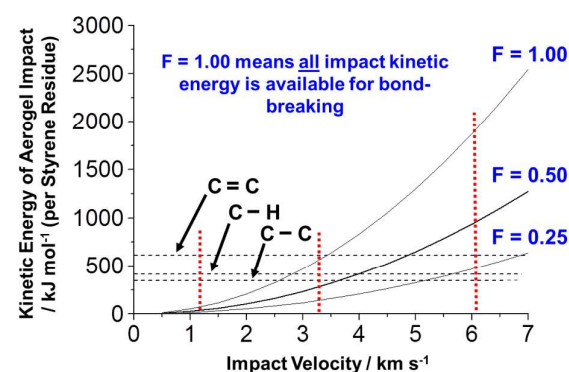


Figure 18. Relationship between kinetic energy of the aerogel impact and the impact velocity of the PPy-coated polystyrene latex. The three curves represent the situations when either 100 %, 50 % or 25 % of the available energy is available for breaking chemical bonds. The energy thresholds for C=C, C-H and C-C bonds are also shown (black dashed lines), while the vertical red lines indicate the impact velocities selected in the LGG aerogel capture experiments.¹⁰⁹

(mineral-based) dust particles were captured within the returned *Stardust* aerogels, remarkably few cometary *organic* grains were captured intact. Instead, much of the organic material was volatilised during the high-speed impact into the aerogel target. However, some particles showed evidence of aliphatic organic content.^{117, 118} Many particles also proved to be coated with disordered carbon, as judged by the carbon D and G bands revealed by *in situ* Raman microscopy studies.¹¹⁷ Accordingly, commercial 20 µm polystyrene latex particles were coated with a polypyrrole overlayer of ~ 20 nm in order to conduct laboratory-based experiments with model organic particles to gain a better understanding of their behaviour during aerogel capture (Figure 15). In these experiments, the ultrathin polypyrrole coating provided a convenient spectroscopic signature. Thus these projectiles are designed to be exquisitely sensitive to thermal ablation when fired into aerogel targets using an LGG (Figure 16).¹⁰⁹ Such core-shell particles survive aerogel capture intact at 1.07 km s⁻¹, as judged by Raman microscopy studies of individual particles located at the end of 'carrot tracks' within the aerogel target (Figure 17). However, this spectroscopic technique confirmed

that surface carbonisation occurred after aerogel capture at approximately 1.95 km s^{-1} , while the observation of D and G Raman bands indicated that the particles were subjected to substantial thermal ablation when captured at or above 3.33 km s^{-1} .¹⁰⁹ Indeed, at an impinging velocity of 6.11 km s^{-1} the mass loss of the captured projectile was estimated to be 84%. Moreover, consideration of the kinetic energies associated with hypervelocity capture under the experimental conditions suggests that these observations are consistent with the mean bond energies required for breaking the C-C, C-H and C=C bonds found in polystyrene, which constitutes more than 99 % of the projectile by mass (Figure 18). These results confirm the hypothesis that many of the organics returned by *Stardust* were substantially thermally ablated during their aerogel capture. Moreover, these findings suggest that relatively low encounter velocities (i.e., $1\text{-}2 \text{ km s}^{-1}$) will be essential for future space missions if organic dust grains originating from comets (or elsewhere) are to be captured intact with minimal thermal ablation.

Conclusions and Prospect

Space science offers a fascinating, if rather esoteric, application for conducting polymer-based particles. The ability to systematically vary their particle size (from 100 nm up to 20 μm) and chemical composition makes them ideal mimics for studying a wide range of carbonaceous, sulfur-rich and silicate-based micro-meteorites. In addition, various mineral grains of astronomical interest such as olivine, pyroxene or pyrrhotite can be readily coated with ultrathin conducting polymer overlayers in order to allow their acceleration up to the hypervelocity regime. Compared to alternative approaches such as metallisation, such organic coatings are cost-effective, have much lower densities and, for many particulate substrates, are contiguous in nature. In most cases the conducting polymer coating simply allows the projectiles to acquire sufficient surface charge to enable electrostatic acceleration, but it has also been shown that this coating can also provide a very convenient spectroscopic signature that enables the extent of thermal ablation of aerogel-captured micro-meteorites to be assessed.

In future work, we intend to examine whether polyaromatic hydrocarbon (PAH) particles can be coated with polypyrrole. If successful, such projectiles should serve as interesting mimics for interstellar dust grains.

Acknowledgements

SPA wishes to thank his many former research group members who have worked so willingly with him over the last two decades in this interdisciplinary research. **MJB** thanks STFC for support over many years. **JKH** thanks STFC, DFG (SPP 1385) and the European Commission. **LAF** thanks EPSRC for post-doctoral support (EP/J018589/1).

Notes and references

‡. Indeed, one of the original objectives in developing synthetic routes to colloidal forms of conducting polymers was to improve the intractability of these fascinating materials.

§. Nevertheless, in our early experiments it was useful to demonstrate that micrometer-sized polystyrene latexes coated with an ultrathin coating of either polypyrrole, PANI or PEDOT generated ionic plasma with essentially the same mass spectra after hypervelocity impacts on metal targets. This confirmed beyond any reasonable doubt that the mass spectra were characteristic of the polystyrene latex cores, rather than the conducting polymer shells. This conclusion was of course expected since the latex cores typically comprise more than 90 % of the projectile by mass, but it is worth emphasizing that other workers had previously erroneously suggested that the conducting polymer coating could dominate the mass spectra obtained from such ionic plasmas, even though this is a relatively minor component of the projectile.

§§. It has recently been shown that millimetre-sized ice particles can be fired at speeds up to 6 km s^{-1} using a two-stage light gas gun. However, it is not currently possible to accelerate micrometre-sized ice particles up to hypervelocities.

1. R. Willstätter and C. W. Moore, *Berichte Der Deutschen Chemischen Gesellschaft*, 1907, **40**, 2665-2689.
2. D. M. Mohilner, W. J. Argersinger and R. N. Adams, *J. Am. Chem. Soc.*, 1962, **84**, 3618.
3. A. Dallolio, G. Dascola, V. Varacca and V. Bocchi, *Comptes Rendus Hebdomadaires Des Seances De L Academie Des Sciences Serie C*, 1968, **267**, 433.
4. D. J. Berets and D. S. Smith, *Transactions of the Faraday Society*, 1968, **64**, 823.
5. Hautiere, F., D. Kuffer and L. T. Yu, *Comptes Rendus Hebdomadaires Des Seances De L Academie Des Sciences Serie C*, 1973, **277**, 1323-1326.
6. H. Shirakawa, E. J. Louis, A. G. Macdiarmid, C. K. Chiang and A. J. Heeger, *J Chem Soc Chem Comm*, 1977, 578-580.
7. J. H. Burroughes, D. D. C. Bradley, A. R. Brown, R. N. Marks, K. Mackay, R. H. Friend, P. L. Burn and A. B. Holmes, *Nature*, 1990, **347**, 539-541.
8. W. L. Ma, C. Y. Yang, X. Gong, K. Lee and A. J. Heeger, *Adv. Funct. Mater.*, 2005, **15**, 1617-1622.
9. M. D. McGehee and A. J. Heeger, *Adv. Mater.*, 2000, **12**, 1655-1668.
10. J. M. Pochan, D. F. Pochan, H. Rommelmann and H. W. Gibson, *Macromolecules*, 1981, **14**, 110-114.
11. S. P. Armes and M. Aldissi, *Polymer*, 1990, **31**, 569-574.
12. J. C. Chiang and A. G. Macdiarmid, *Synthetic Metals*, 1986, **13**, 193-205.
13. Q. B. Pei, G. Zuccarello, M. Ahlskog and O. Inganas, *Polymer*, 1994, **35**, 1347-1351.
14. S. P. Armes, *Synthetic Metals*, 1987, **20**, 365-371.
15. S. P. Armes and J. F. Miller, *Synthetic Metals*, 1988, **22**, 385-393.
16. R. Corradi and S. P. Armes, *Synthetic Metals*, 1997, **84**, 453-454.
17. S. Maeda and S. P. Armes, *J. Mater. Chem.*, 1994, **4**, 935-942.
18. K. C. Khulbe, R. S. Mann and C. P. Khulbe, *Journal of Polymer Science: Polymer Chemistry Edition*, 1982, **20**, 1089-1095.
19. R. B. Bjorklund, *Journal of the Chemical Society-Faraday Transactions I*, 1987, **83**, 1507-1514.

20. M. T. Gill, S. E. Chapman, C. L. DeArmitt, F. L. Baines, C. M. Dadswell, J. G. Stamper, G. A. Lawless, N. C. Billingham and S. P. Armes, *Synthetic Metals*, 1998, **93**, 227-233.
21. S. P. Armes and B. Vincent, *J Chem Soc Chem Comm*, 1987, 288-290.
22. P. M. Beadle, S. P. Armes, S. J. Greaves and J. F. Watts, *Langmuir*, 1996, **12**, 1784-1788.
23. M. R. Simmons, P. A. Chaloner, S. P. Armes, S. J. Greaves and J. F. Watts, *Langmuir*, 1998, **14**, 611-618.
24. M. Morgan, L. A. Fielding and S. P. Armes, *Colloid Polymer Science*, 2013, **291**, 77-86.
25. Z. Zha, X. Yue, Q. Ren and Z. Dai, *Adv. Mater.*, 2013, **25**, 777-782.
26. K. Yang, H. Xu, L. Cheng, C. Sun, J. Wang and Z. Liu, *Adv. Mater.*, 2012, **24**, 5586-5592.
27. K. M. Au, Z. Lu, S. J. Matcher and S. P. Armes, *Adv. Mater.*, 2011, **23**, 5792-5795.
28. K. M. Au, Z. Lu, S. J. Matcher and S. P. Armes, *Biomaterials*, 2013, **34**, 8925-8940.
29. K. M. Au, M. Chen, S. P. Armes and N. Zheng, *Chem. Commun.*, 2013, **49**, 10525-10527.
30. A. Ramanaviciene, A. Kausaite, S. Tautkus and A. Ramanavicius, *Journal of Pharmacy and Pharmacology*, 2007, **59**, 311-315.
31. P. J. Tarcha, D. Misun, D. Finley, M. Wong and J. J. Donovan, *Acs Symposium Series*, 1992, **492**, 347-367.
32. M. R. Pope, S. P. Armes and P. J. Tarcha, *Bioconjugate Chem.*, 1996, **7**, 436-444.
33. S. P. Armes, M. Aldissi, G. C. Idzorek, P. W. Keaton, L. J. Rowton, G. L. Stradling, M. T. Collopy and D. B. McColl, *J. Colloid Interface Sci.*, 1991, **141**, 119-126.
34. M. J. Burchell, M. J. Cole, J. A. M. McDonnell and J. C. Zarnecki, *Measurement Science & Technology*, 1999, **10**, 41-50.
35. C. K. Ober, K. P. Lok and M. L. Hair, *Journal of Polymer Science Part C-Polymer Letters*, 1985, **23**, 103-108.
36. C. Perruchot, M. M. Chehimi, M. Delamar, S. F. Lascelles and S. P. Armes, *Langmuir*, 1996, **12**, 3245-3251.
37. S. F. Lascelles and S. P. Armes, *Adv. Mater.*, 1995, **7**, 864-866.
38. S. F. Lascelles and S. P. Armes, *J. Mater. Chem.*, 1997, **7**, 1339-1347.
39. S. F. Lascelles, S. P. Armes, P. A. Zhdan, S. J. Greaves, A. M. Brown, J. F. Watts, S. R. Leadley and S. Y. Luk, *J. Mater. Chem.*, 1997, **7**, 1349-1355.
40. J. Ormond-Prout, D. Dupin, S. P. Armes, N. J. Foster and M. J. Burchell, *J. Mater. Chem.*, 2009, **19**, 1433-1442.
41. S. Fujii, S. P. Armes, R. Jeans, R. Devonshire, S. Warren, S. L. McArthur, M. J. Burchell, F. Postberg and R. Srama, *Chem. Mater.*, 2006, **18**, 2758-2765.
42. M. A. Khan, S. P. Armes, C. Perruchot, H. Ouamara, M. M. Chehimi, S. J. Greaves and J. F. Watts, *Langmuir*, 2000, **16**, 4171-4179.
43. M. A. Khan and S. P. Armes, *Langmuir*, 1999, **15**, 3469-3475.
44. C. Barthet, S. P. Armes, S. F. Lascelles, S. Y. Luk and H. M. E. Stanley, *Langmuir*, 1998, **14**, 2032-2041.
45. C. Barthet, S. P. Armes, M. M. Chehimi, C. Bilem and M. Omastova, *Langmuir*, 1998, **14**, 5032-5038.
46. D. B. Cairns, M. A. Khan, C. Perruchot, A. Riede and S. P. Armes, *Chem. Mater.*, 2003, **15**, 233-239.
47. S. Maeda and S. P. Armes, *J. Colloid Interface Sci.*, 1993, **159**, 257-259.
48. S. F. Lascelles, G. P. McCarthy, M. D. Butterworth and S. P. Armes, *Colloid Polymer Science*, 1998, **276**, 893-902.
49. M. G. Han and S. P. Armes, *J. Colloid Interface Sci.*, 2003, **262**, 418-427.
50. S. Maeda, M. Gill, S. P. Armes and I. W. Fletcher, *Langmuir*, 1995, **11**, 1899-1904.
51. M. D. Butterworth, R. Corradi, J. Johal, S. F. Lascelles, S. Maeda and S. P. Armes, *J. Colloid Interface Sci.*, 1995, **174**, 510-517.
52. J. K. Hillier, Z. Sternovsky, S. P. Armes, L. A. Fielding, F. Postberg, S. Bugiel, K. Drake, R. Srama, A. T. Kearsley and M. Trieloff, *Planet. Space Sci.*, 2014, **97**, 9-22.
53. F. Postberg, J. K. Hillier, S. P. Armes, S. Bugiel, A. Butterworth, D. Dupin, L. A. Fielding, S. Fujii, Z. Gainsforth, E. Gruen, Y. W. Li, R. Srama, V. Sterken, J. Stodolna, M. Trieloff, A. Westphal, C. Achilles, C. Allen, A. Ansari, S. Bajt, N. Bassim, R. K. Bastien, H. A. Bechtel, J. Borg, F. Brenker, J. Bridges, D. E. Brownlee, M. Burchell, M. Burghammer, H. Changela, P. Cloetens, A. Davis, R. Doll, C. Floss, G. Flynn, D. Frank, P. R. Heck, P. Hoppe, G. Huss, J. Huth, A. Kearsley, A. J. King, B. Lai, J. Leitner, L. Lemelle, A. Leonard, H. Leroux, R. Lettieri, W. Marchant, L. R. Nittler, R. Oglione, W. J. Ong, M. C. Price, S. A. Sandford, J. A. S. Tressaras, S. Schmitz, T. Schoonjans, K. Schreiber, G. Silversmit, A. Simionovici, V. A. Sole, F. Stadermann, T. Stephan, R. M. Stroud, S. Sutton, P. Tsou, A. Tsuchiyama, T. Tyliczszak, B. Vekemans, L. Vincze, D. Zevin and M. E. Zolensky, *Meteorit. Planet. Sci.*, 2014, **49**, 1666-1679.
54. S. Maeda and S. P. Armes, *Chem. Mater.*, 1995, **7**, 171-178.
55. S. Maeda and S. P. Armes, *Synthetic Metals*, 1995, **69**, 499-500.
56. Y. W. Li, S. Bugiel, M. Trieloff, J. K. Hillier, F. Postberg, M. C. Price, A. Shu, K. Fiege, L. A. Fielding, S. P. Armes, Y. Y. Wu, E. Grün and R. Srama, *Meteorit. Planet. Sci.*, 2014, **49**, 1375-1387.
57. J. R. Lovett, L. A. Fielding, S. P. Armes and R. Buxton, *Adv. Funct. Mater.*, 2014, **24**, 1290-1299.
58. S. P. Armes, S. Gottesfeld, J. G. Beery, F. Garzon and S. F. Agnew, *Polymer*, 1991, **32**, 2325-2330.
59. Z. Huang, P.-C. Wang, A. G. MacDiarmid, Y. Xia and G. Whitesides, *Langmuir*, 1997, **13**, 6480-6484.
60. P. J. Wozniakiewicz, M. C. Price, S. P. Armes, M. J. Burchell, M. J. Cole, L. A. Fielding, J. K. Hillier and J. R. Lovett, *Meteorit. Planet. Sci.*, 2014, **49**, 1929-1947.
61. S. P. Armes and M. Aldissi, *J Chem Soc Chem Comm*, 1989, 88-89.
62. M. Mumtaz, S. Lecommandoux, E. Cloutet and H. Cramail, *Langmuir*, 2008, **24**, 11911-11920.
63. M. Gill, J. Mykytiuk, S. P. Armes, J. L. Edwards, T. Yeates, P. J. Moreland and C. Mollett, *J. Chem. Soc. Chem. Commun.*, 1992, 108-109.
64. M. G. Han and S. P. Armes, *Langmuir*, 2003, **19**, 4523-4526.
65. J. K. Hillier, S. Sestak, S. F. Green, F. Postberg, R. Srama and M. Trieloff, *Planet. Space Sci.*, 2009, **57**, 2081-2086.

66. M. J. Burchell, M. J. Willis, S. P. Armes, M. A. Khan, M. J. Percy and C. Perruchot, *Planet. Space Sci.*, 2002, **50**, 1025-1035.
67. J. K. Hillier, F. Postberg, S. Sestak, R. Srama, S. Kempf, M. Tieloff, Z. Sternovsky and S. F. Green, *Journal of Geophysical Research-Planets*, 2012, **117**.
68. K. Fiege, M. Tieloff, J. K. Hillier, M. Guglielmino, F. Postberg, R. Srama, S. Kempf and J. Blum, *Icarus*, 2014, **241**, 336-345.
69. R. Srama, W. Woiwode, F. Postberg, S. P. Armes, S. Fujii, D. Dupin, J. Ormond-Prout, Z. Sternovsky, S. Kempf, G. Moragas-Klostermeyer, A. Mocker and E. Grun, *Rapid Commun. Mass Spectrom.*, 2009, **23**, 3895-3906.
70. B. J. Goldsworthy, M. J. Burchell, M. J. Cole, S. P. Armes, M. A. Khan, S. F. Lascelles, S. F. Green, J. A. M. McDonnell, R. Srama and S. W. Bigger, *Astron. Astrophys.*, 2003, **409**, 1151-1167.
71. H. Dietzel, G. Neukum and P. Rauser, *Journal of Geophysical Research*, 1972, **77**, 1375-&.
72. M. A. Khan and S. P. Armes, *Adv. Mater.*, 2000, **12**, 671.
73. R. Srama, T. J. Ahrens, N. Altobelli, S. Auer, J. G. Bradley, M. Burton, V. V. Dikarev, T. Economou, H. Fechtig, M. Gorlich, M. Grande, A. Graps, E. Grun, O. Havnes, S. Helfert, M. Horanyi, E. Igenbergs, E. K. Jessberger, T. V. Johnson, S. Kempf, A. V. Krivov, H. Kruger, A. Mocker-Ahlreep, G. Moragas-Klostermeyer, P. Lamy, M. Landgraf, D. Linkert, G. Linkert, F. Lura, J. A. M. McDonnell, D. Mohlmann, G. E. Morfill, M. Muller, M. Roy, G. Schafer, G. Schlotzhauer, G. H. Schwehm, F. Spahn, M. Stubig, J. Vestka, V. Tschernjowski, A. J. Tuzzolino, R. Wasch and H. A. Zook, *Space Science Reviews*, 2004, **114**, 465-518.
74. Z. Sternovsky, K. Amyx, G. Bano, M. Landgraf, M. Horanyi, S. Knappmiller, S. Robertson, E. Grün, R. Srama and S. Auer, *Rev. Sci. Instrum.*, 2007, **78**, 014501.
75. A. Mocker, S. Bugiel, S. Auer, G. Baust, A. Colette, K. Drake, K. Fiege, E. Grun, F. Heckmann, S. Helfert, J. Hillier, S. Kempf, G. Matt, T. Mellert, T. Munsat, K. Otto, F. Postberg, H. P. Roser, A. Shu, Z. Sternovsky and R. Srama, *Rev. Sci. Instrum.*, 2011, **82**.
76. A. Shu, A. Collette, K. Drake, E. Gruen, M. Horanyi, S. Kempf, A. Mocker, T. Munsat, P. Northway, R. Srama, Z. Sternovsky and E. Thomas, *Rev. Sci. Instrum.*, 2012, **83**, 075108.
77. K. A. Otto, R. Srama, S. Auer, S. Bugiel, E. Grun, S. Kempf and J. F. Xie, *Nucl. Instrum. Methods Phys. Res. Sect. A-Accel. Spectrom. Dect. Assoc. Equip.*, 2013, **729**, 841-848.
78. R. Srama and S. Auer, *Measurement Science & Technology*, 2008, **19**.
79. R. Srama, S. Kempf, G. Moragas-Klostermeyer, M. Landgraf, S. Helfert, Z. Sternovsky, M. Rachev, E. Gruen and Esa, in *Workshop on Dust in Planetary Systems*, 2007, vol. 643, pp. 209-212.
80. B. A. Mamyrin, V. I. Karataev, D. V. Shmikk and V. A. Zagulin, *Zhurnal Eksperimentalnoi I Teoreticheskoi Fiziki*, 1973, **64**, 82-89.
81. K. Hornung and J. Kissel, *Astron. Astrophys.*, 1994, **291**, 324-336.
82. A. Mocker, E. Gruen, Z. Sternovsky, K. Drake, S. Kempf, K. Hornung and R. Srama, *Journal of Applied Physics*, 2012, **112**.
83. E. M. Mellado, K. Hornung, R. Srama, J. Kissel, S. P. Armes and S. Fujii, *International Journal of Impact Engineering*, 2011, **38**, 486-494.
84. B. J. Goldsworthy, M. J. Burchell, M. J. Cole, S. F. Green, M. R. Leese, N. McBride, J. A. M. McDonnell, M. Muller, E. Grun, R. Srama, S. P. Armes and M. A. Khan, in *Exploration of Small Solar System Objects: Past, Present and Future*, ed. N. Thomas, 2002, vol. 29, pp. 1139-1144.
85. D. P. Cruikshank, in *From Stardust to Planetesimals*, ed. Y. J. Pendleton, 1997, vol. 122, p. 315.
86. J. R. Cronin, S. Pizzarello and D. P. Cruikshank, in *Meteorites and the Early Solar System*, eds. J. F. Kerridge and M. S. Matthews, 1988, pp. 819-857.
87. D. P. Cruikshank, *Advances in Space Research*, 1989, **9**, 65-71.
88. K. L. Thomas, L. P. Keller, G. E. Blanford and D. S. McKay, *Meteoritics*, 1992, **27**, 296-297.
89. C. Sagan and B. N. Khare, *Nature*, 1979, **277**, 102-107.
90. D. P. Cruikshank, T. L. Roush, M. J. Bartholomew, T. R. Geballe, Y. J. Pendleton, S. M. White, J. F. Bell, J. K. Davies, T. C. Owen, C. de Bergh, D. J. Tholen, M. P. Bernstein, R. H. Brown, K. A. Tryka and C. M. Dalle Ore, *Icarus*, 1998, **135**, 389-407.
91. R. H. Brown, D. P. Cruikshank, Y. Pendleton and G. J. Veeder, *Science*, 1997, **276**, 937-939.
92. E. Dwek, R. G. Arendt, D. J. Fixsen, T. J. Sodroski, N. Odegard, J. L. Weiland, W. T. Reach, M. G. Hauser, T. Kelsall, S. H. Moseley, R. F. Silverberg, R. A. Shafer, J. Ballester, D. Bazell and R. Isaacman, *Astrophysical Journal*, 1997, **475**, 565-579.
93. L. J. Allamandola, S. A. Sandford and B. Wopenka, *Science*, 1987, **237**, 56-59.
94. A. J. Westphal, R. M. Stroud, H. A. Bechtel, F. E. Brenker, A. L. Butterworth, G. J. Flynn, D. R. Frank, Z. Gainsforth, J. K. Hillier, F. Postberg, A. S. Simionovici, V. J. Sterken, L. R. Nittler, C. Allen, D. Anderson, A. Ansari, S. Bajt, R. K. Bastien, N. Bassim, J. Bridges, D. E. Brownlee, M. Burchell, M. Burghammer, H. Changela, P. Cloetens, A. M. Davis, R. Doll, C. Floss, E. Gruen, P. R. Heck, P. Hoppe, B. Hudson, J. Huth, A. Kearsley, A. J. King, B. Lai, J. W. Leitner, L. Lemelle, A. Leonard, H. Leroux, R. Lettieri, W. Marchant, R. Ogiore, W. J. Ong, M. C. Price, S. A. Sandford, J.-A. S. Tresseras, S. Schmitz, T. Schoonjans, K. Schreiber, G. Silversmit, V. A. Sole, R. Srama, F. Stadermann, T. Stephan, J. Stodolna, S. Sutton, M. Tieloff, P. Tsou, T. Tyliczszak, B. Vekemans, L. Vincze, J. Von Korff, N. Wordsworth, D. Zevin, M. E. Zolensky and D. Stardust Home, *Science*, 2014, **345**, 786-791.
95. M. J. Burchell and S. P. Armes, *Rapid Commun. Mass Spectrom.*, 2011, **25**, 543-550.
96. J. Kissel and F. R. Krueger, *Rapid Commun. Mass Spectrom.*, 2001, **15**, 1713-1718.
97. F. Postberg, S. Kempf, D. Rost, T. Stephan, R. Srama, M. Tieloff, A. Mocker and M. Goerlich, *Planet. Space Sci.*, 2009, **57**, 1359-1374.
98. M. J. Gaffey, J. F. Bell, R. H. Brown, T. H. Burbine, J. L. Piatek, K. L. Reed and D. A. Chaky, *Icarus*, 1993, **106**, 573-602.
99. M. E. Zolensky, T. J. Zega, H. Yano, S. Wirick, A. J. Westphal, M. K. Weisberg, I. Weber, J. L. Warren, M. A. Velbel, A. Tsuchiyama, P. Tsou, A. Toppani, N. Tomioka, K. Tomeoka, N. Teslich, M. Taheri, J. Susini, R. Stroud, T. Stephan, F. J. Stadermann, C. J. Snead, S. B. Simon, A. Simionovici, T. H. See, F. Robert, F. J. M. Rietmeijer, W. Rao, M. C. Perronnet, D. A. Papanastassiou, K. Okudaira, K. Ohsumi, I. Ohnishi, K. Nakamura-Messenger, T. Nakamura, S. Mostefaoui, T. Mikouchi, A. Meibom, G. Matrajt, M. A. Marcus, H. Leroux, L. Lemelle, L. Le, A. Lanzirotti, F. Langenhorst, A. N. Krot, L. P. Keller, A. T.

- Kearsley, D. Joswiak, D. Jacob, H. Ishii, R. Harvey, K. Hagiya, L. Grossman, J. N. Grossman, G. A. Graham, M. Gounelle, P. Gillet, M. J. Genge, G. Flynn, T. Ferroir, S. Fallon, D. S. Ebel, Z. R. Dai, P. Cordier, B. Clark, M. Chi, A. L. Butterworth, D. E. Brownlee, J. C. Bridges, S. Brennan, A. Brearley, J. P. Bradley, P. Bleuuet, P. A. Bland and R. Bastien, *Science*, 2006, **314**, 1735-1739.
100. K. Nagashima, A. N. Krot and H. Yurimoto, *Nature*, 2004, **428**, 921-924.
101. E. Gruen, H. Fechtig, R. H. Giese, J. Kissel, L. D. Linkert, J. A. M. McDonnell, G. E. Morfill, G. Schwehm and H. A. Zook, *European Space Agency, (Special Publication) ESA SP*, 1983, 227-241.
102. E. Grun, H. Fechtig, M. S. Hanner, J. Kissel, B. A. Lindblad, D. Linkert, D. Maas, G. E. Morfill and H. A. Zook, *Space Science Reviews*, 1992, **60**, 317-340.
103. J. R. Goller and E. Grun, *Planet. Space Sci.*, 1989, **37**, 1197-1206.
104. M. J. Burchell, M. J. Cole, S. F. Lascelles, M. A. Khan, C. Barthet, S. A. Wilson, D. B. Cairns and S. P. Armes, *Journal of Physics D-Applied Physics*, 1999, **32**, 1719-1728.
105. W. D. Crozier and W. Hume, *Journal of Applied Physics*, 1957, **28**, 892-894.
106. L. A. Glenn, in *Shock waves in condensed matter*, eds. S. C. Schmidt and N. C. Holmes, Elsevier Science Publishers, Amsterdam, 1987, pp. 653-656.
107. B. Lexow, M. Wickert, K. Thoma, F. Schaefer, M. H. Poelchau and T. Kenkmann, *Meteorit. Planet. Sci.*, 2013, **48**, 3-7.
108. T. Moritoh, N. Kawai, K. G. Nakamura and K.-I. Kondo, in *Shock compression of condensed matter*, eds. M. D. Furnish, N. N. Thadhani and Y. Horie, American Institute of Physics, New York, 2001, pp. 1204-1207.
109. M. J. Burchell, N. J. Foster, J. Ormond-Prout, D. Dupin and S. P. Armes, *Meteorit. Planet. Sci.*, 2009, **44**, 1407-1420.
110. D. E. Brownlee, P. Tsou, J. D. Anderson, M. S. Hanner, R. L. Newburn, Z. Sekanina, B. C. Clark, F. Horz, M. E. Zolensky, J. Kissel, J. A. M. McDonnell, S. A. Sandford and A. J. Tuzzolino, *Journal of Geophysical Research-Planets*, 2003, **108**.
111. D. Brownlee, P. Tsou, J. Aleon, C. M. O. D. Alexander, T. Araki, S. Bajt, G. A. Baratta, R. Bastien, P. Bland, P. Bleuuet, J. Borg, J. P. Bradley, A. Brearley, F. Brenker, S. Brennan, J. C. Bridges, N. D. Browning, J. R. Brucato, E. Bullock, M. J. Burchell, H. Busemann, A. Butterworth, M. Chaussidon, A. Chevront, M. Chi, M. J. Cintala, B. C. Clark, S. J. Clemett, G. Cody, L. Colangeli, G. Cooper, P. Cordier, C. Daghlian, Z. Dai, L. D'Hendecourt, Z. Djouadi, G. Dominguez, T. Duxbury, J. P. Dworkin, D. S. Ebel, T. E. Economou, S. Fakra, S. A. J. Fairey, S. Fallon, G. Ferrini, T. Ferroir, H. Fleckenstein, C. Floss, G. Flynn, I. A. Franchi, M. Fries, Z. Gainsforth, J. P. Gallien, M. Genge, M. K. Gilles, P. Gillet, J. Gilmore, D. P. Glavin, M. Gounelle, M. M. Grady, G. A. Graham, P. G. Grant, S. F. Green, F. Grossemy, L. Grossman, J. N. Grossman, Y. Guan, K. Hagiya, R. Harvey, P. Heck, G. F. Herzog, P. Hoppe, F. Hoerz, J. Huth, I. D. Hutcheon, K. Ignatyev, H. Ishii, M. Ito, D. Jacob, C. Jacobsen, S. Jacobsen, S. Jones, D. Joswiak, A. Jurewicz, A. T. Kearsley, L. P. Keller, H. Khodja, A. L. D. Kilcoyne, J. Kissel, A. Krot, F. Langenhorst, A. Lanzirotti, L. Le, L. A. Leshin, J. Leitner, L. Lemelle, H. Leroux, M.-C. Liu, K. Luening, I. Lyon, G. MacPherson, M. A. Marcus, K. Marhas, B. Marty, G. Matrajt, K. McKeegan, A. Meibom, V. Mennella, K. Messenger, S. Messenger, T. Mikouchi, S. Mostefaoui, T. Nakamura, T. Nakano, M. Newville, L. R. Nittler, I. Ohnishi, K. Ohsumi, K. Okudaira, D. A. Papanastassiou, R. Palma, M. E. Palumbo, R. O. Pepin, D. Perkins, M. Perronnet, P. Pianetta, W. Rao, F. J. M. Rietmeijer, F. Robert, D. Rost, A. Rotundi, R. Ryan, S. A. Sandford, C. S. Schwandt, T. H. See, D. Schlutter, J. Sheffield-Parker, A. Simionovici, S. Simon, I. Sitnitsky, C. J. Snead, M. K. Spencer, F. J. Stadermann, A. Steele, T. Stephan, R. Stroud, J. Susini, S. R. Sutton, Y. Suzuki, M. Taheri, S. Taylor, N. Teslich, K. Tomeoka, N. Tomioka, A. Toppani, J. M. Trigo-Rodriguez, D. Troadec, A. Tsuchiyama, A. J. Tuzzolino, T. Tyliczszak, K. Uesugi, M. Velbel, J. Vellenga, E. Vicenzi, L. Vincze, J. Warren, I. Weber, M. Weisberg, A. J. Westphal, S. Wirick, D. Wooden, B. Wopenka, P. Wozniakiewicz, I. Wright, H. Yabuta, H. Yano, E. D. Young, R. N. Zare, T. Zega, K. Ziegler, L. Zimmerman, E. Zinner and M. Zolensky, *Science*, 2006, **314**, 1711-1716.
112. M. J. Burchell, G. Graham and A. Kearsley, in *Annual Review of Earth and Planetary Sciences*, 2006, vol. 34, pp. 385-418.
113. F. Hoerz, R. Bastien, J. Borg, J. P. Bradley, J. C. Bridges, D. E. Brownlee, M. J. Burchell, M. Chi, M. J. Cintala, Z. R. Dai, Z. Djouadi, G. Dominguez, T. E. Economou, S. A. J. Fairey, C. Floss, I. A. Franchi, G. A. Graham, S. F. Green, P. Heck, P. Hoppe, J. Huth, H. Ishii, A. T. Kearsley, J. Kissel, J. Leitner, H. Leroux, K. Marhas, K. Messenger, C. S. Schwandt, T. H. See, C. Snead, F. J. Stadermann, T. Stephan, R. Stroud, N. Teslich, J. M. Trigo-Rodriguez, A. J. Tuzzolino, D. Troadec, P. Tsou, J. Warren, A. Westphal, P. Wozniakiewicz, I. Wright and E. Zinner, *Science*, 2006, **314**, 1716-1719.
114. M. J. Burchell, S. A. J. Fairey, P. Wozniakiewicz, D. E. Brownlee, F. Hoerz, A. T. Kearsley, T. H. See, P. Tsou, A. Westphal, S. F. Green, J. M. Trigo-Rodriguez and G. Dominguez, *Meteorit. Planet. Sci.*, 2008, **43**, 23-40.
115. J. M. Trigo-Rodriguez, G. Dominguez, M. J. Burchell, F. Hoerz and J. Llorca, *Meteorit. Planet. Sci.*, 2008, **43**, 75-86.
116. A. J. Westphal, D. Anderson, A. L. Butterworth, D. R. Frank, R. Lettieri, W. Marchant, J. Von Korff, D. Zevin, A. Ardizzone, A. Campanile, M. Capraro, K. Courtney, M. N. Criswell, III, D. Crumpler, R. Cwik, F. J. Gray, B. Hudson, G. Imada, J. Karr, L. L. W. Wah, M. Mazzucato, P. G. Motta, C. Rigamonti, R. C. Spencer, S. B. Woodrough, I. C. Santoni, G. Sperry, J.-N. Terry, N. Wordsworth, T. Yahnke, Sr., C. Allen, A. Ansari, S. Bajt, R. K. Bastien, N. Bassim, H. A. Bechtel, J. Borg, F. E. Brenker, J. Bridges, D. E. Brownlee, M. Burchell, M. Burghammer, H. Changela, P. Cloetens, A. M. Davis, R. Doll, C. Floss, G. Flynn, Z. Gainsforth, E. Gruen, P. R. Heck, J. K. Hillier, P. Hoppe, J. Huth, B. Hvide, A. Kearsley, A. J. King, B. Lai, J. Leitner, L. Lemelle, H. Leroux, A. Leonard, L. R. Nittler, R. Oglione, W. J. Ong, F. Postberg, M. C. Price, S. A. Sandford, J.-A. S. Tresseras, S. Schmitz, T. Schoonjans, G. Silversmit, A. S. Simionovici, V. A. Sole, R. Srama, T. Stephan, V. J. Sterken, J. Stodolna, R. M. Stroud, S. Sutton, M. Tieloff, P. Tsou, A. Tsuchiyama, T. Tyliczszak, B. Vekemans, L. Vincze and M. E. Zolensky, *Meteorit. Planet. Sci.*, 2014, **49**, 1509-1521.
117. S. A. Sandford, J. Aleon, C. M. O. D. Alexander, T. Araki, S. Bajt, G. A. Baratta, J. Borg, J. P. Bradley, D. E. Brownlee, J. R. Brucato, M. J. Burchell, H. Busemann, A. Butterworth, S. J.

Clemett, G. Cody, L. Colangeli, G. Cooper, L. D'Hendecourt, Z. Djouadi, J. P. Dworkin, G. Ferrini, H. Fleckenstein, G. J. Flynn, I. A. Franchi, M. Fries, M. K. Gilles, D. P. Glavin, M. Gounelle, F. Grossemy, C. Jacobsen, L. P. Keller, A. L. D. Kilcoyne, J. Leitner, G. Matrajt, A. Meibom, V. Mennella, S. Mostefaoui, L. R. Nittler, M. E. Palumbo, D. A. Papanastassiou, F. Robert, A. Rotundi, C. J. Snead, M. K. Spencer, F. J. Stadermann, A. Steele, T. Stephan, P. Tsou, T. Tyliczszak, A. J. Westphal, S. Wirick, B. Wopenka, H. Yabuta, R. N. Zare and M. E. Zolensky, *Science*, 2006, **314**, 1720-1724.

118. L. P. Keller, S. Bajt, G. A. Baratta, J. Borg, J. P. Bradley, D. E. Brownlee, H. Busemann, J. R. Brucato, M. Burchell, L. Colangeli, L. d'Hendecourt, Z. Djouadi, G. Ferrini, G. Flynn, I. A. Franchi, M. Fries, M. M. Grady, G. A. Graham, F. Grossemy, A. Kearsley, G. Matrajt, K. Nakamura-Messenger, V. Mennella, L. Nittler, M. E. Palumbo, F. J. Stadermann, P. Tsou, A. Rotundi, S. A. Sandford, C. Snead, A. Steele, D. Wooden and M. Zolensky, *Science*, 2006, **314**, 1728-1731.

Vitae

Lee A. Fielding



Dr. Lee A. Fielding obtained a MChem in Chemistry with first class honours from the University of Sheffield in 2008, which was followed by a PhD in 2012 on the synthesis, characterisation and applications of colloidal nanocomposite particles from the same institution with Prof. Armes. Dr. Fielding then worked as a Postdoctoral Researcher in the group of Prof. Armes working on the preparation of bespoke colloidal particles via RAFT dispersion polymerization, in part for occlusion within inorganic host crystals. He took up a Lectureship in the School of Materials at the University of Manchester in September 2015.

Jon K. Hillier



Dr. Jon K. Hillier received his PhD in Physics from the University of Kent in 2003. After a brief foray into Computer Science at Oxford University, he entered the field of Cosmic Dust research, working at the Open University on the *Cassini* Cosmic Dust Analyser. Here he also developed methods for producing metal-coated cosmic dust analogue particles. Between 2011 and 2014 he worked at the University of Heidelberg, Germany, on the *Stardust* Interstellar Preliminary Examination team. He is currently a Marie-Curie IntraEuropean Research Fellow at the University of Kent, producing novel liquid-filled microparticles as analogues of volatile cosmic dust grains.

Mark J. Burchell



Prof. Burchell graduated with a BSc in Physics from Birmingham in 1981 and a PhD in Particle Physics from Imperial College in 1986. He held post-doctoral positions at Imperial and Univ. California Santa Cruz, followed by a CERN Fellowship. He was appointed as a Lecturer in Space Science at the University of Kent in 1993, was promoted to Professor in 2007 and to Dean of Science in 2010. He has published >200 refereed journal papers in physics and space science, with >5,200 citations and a H-index of 35. His research interests include cosmic dust, asteroids, comets, impact phenomena and astrobiology.

Steven P. Armes



Prof. Armes graduated from Bristol University (BSc 1983, PhD 1987). He worked as a post-doc at Los Alamos National Laboratory for two years before taking up a Lectureship at Sussex University in 1989. He was promoted to Professor in 2000 and joined the University of Sheffield in 2004. He has published >500 papers (H-index 93) and was elected as a Fellow of the Royal Society in 2014. Polypyrrole has always been his favourite polymer and he received the 2014 RSC Interdisciplinary Prize for the subject of this review article. Other research interests include block copolymer self-assembly and controlled-structure water-soluble polymers.

Table of contents graphic

